Available online at www.sciencedirect.com
ScienceDirect
Chinese Journal of Natural Medicines 2020, **18**(8): 594-605
doi: 10.1016/S1875-5364(20)30071-6
Chinese Journal of Natural Medicines

•Special topic•

Identification of medicinal plants within the Apocynaceae family using ITS2 and *psbA-trnH* barcodes

LV Ya-Na[1, 2Δ], YANG Chun-Yong[1, 2Δ], SHI Lin-Chun[3, 4], ZHANG Zhong-Lian[1, 2], XU An-Shun[1, 2], ZHANG Li-Xia[1, 2, 4], LI Xue-Lan[1, 2, 4], LI Hai-Tao[1, 2, 4*]

[1] *Yunnan Branch, Institute of Medicinal Plant Development, Chinese Academy of Medical Sciences & Peking Union Medical College, Jinghong 666100, China;*
[2] *Key Laborartory of Dai and Southern Medicine of Xishuangbanna Dai Autonomous Prefecture, Jinghong 666100, China;*
[3] *Key Lab of Chinese Medicine Resources Conservation, State Administration of Traditional Chinese Medicine of the People's Republic of China, Institute of Medicinal Plant Development, Chinese Academy of Medical Sciences & Peking Union Medical College, Beijing, 100193, China;*
[4] *Engineering Research Center of Tradition Chinese Medicine Resource, Ministry of Education, Institute of Medicinal Plant Development, Chinese Academy of Medical Sciences & Peking Union Medical College, Beijing, 100193, China*

Available online 20 Aug., 2020

[ABSTRACT] To ensure the safety of medications, it is vital to accurately authenticate species of the Apocynaceae family, which is rich in poisonous medicinal plants. We identified Apocynaceae species by using nuclear internal transcribed spacer 2 (ITS2) and *psbA-trnH* based on experimental data. The identification ability of ITS2 and *psbA-trnH* was assessed using specific genetic divergence, BLAST1, and neighbor-joining trees. For DNA barcoding, ITS2 and *psbA-trnH* regions of 122 plant samples of 31 species from 19 genera in the Apocynaceae family were amplified. The PCR amplification for ITS2 and *psbA-trnH* sequences was 100%. The sequencing success rates for ITS2 and *psbA-trnH* sequences were 81% and 61%, respectively. Additional data involved 53 sequences of the ITS2 region and 38 sequences of the *psbA-trnH* region were downloaded from GenBank. Moreover, the analysis showed that the interspecific divergence of Apocynaceae species was greater than its intra-specific variations. The results indicated that, using the BLAST1 method, ITS2 showed a high identification efficiency of 97% and 100% of the samples at the species and genus levels, respectively, *via* BLAST1, and *psbA-trnH* successfully identified 95% and 100% of the samples at the species and genus levels, respectively. The barcode combination of ITS2/*psbA-trnH* successfully identified 98% and 100% of samples at the species and genus levels, respectively. Subsequently, the neighbor joining tree method also showed that barcode ITS2 and *psbA-trnH* could distinguish among the species within the Apocynaceae family. ITS2 is a core barcode and *psbA-trnH* is a supplementary barcode for identifying species in the Apocynaceae family. These results will help to improve DNA barcoding reference databases for herbal drugs and other herbal raw materials.

[KEY WORDS] Apocynaceae; DNA barcoding; ITS2; *psbA-trnH*; Species identification
[CLC Number] R282.5 **[Document code]** A **[Article ID]** 2095-6975(2020)08-0594-12

Introduction

The Apocynaceae family comprises more than 2000 species that are distributed mostly in tropical regions and have been recorded in 63 volumes of the *Flora of China*. This family has great importance due to its use in food, its economic implications related to medicinal and ornamental applications, and its toxicological aspects [1]. The plants of the Apocynaceae family are rich in alkaloids, terpenoids, steroids, flavonoids, glycosides, simple phenols, lactones, and hydrocarbons [2-5]. Some members of the Apocynaceae family are widely used ethnomedicines around the world. Table S1 summarizes the ethnomedicinal importance of various plants of family Apocynaceae. It has been reported that crude extracts and single compound(s) isolated from various members of the Apocynaceae family possess a wide range of bioactivities, in-

[Received on] 19-Apr.-2020
[Research funding] This work was supported by the CAMS Initiative for Innovative Medicine (No. 2016-12M-2-003) and the Special Subsidies for Public Health Services of TCM ("The National Survey of TCM Resources", DSS, MOF; No. 66/2017). .
[*]**Corresponding author]** E-mail: 15894318030@126.com
[Δ]These authors contributed equally to this work.
These authors have no conflict of interest to declare.

cluding antioxidant activity, anti-inflammatory/analgesic activity, anticancer/cytotoxic activity, antimicrobial activity, and cardioprotective activity [6-8]. The significant anti-inflammatory activity and potent cytotoxic activity of *Ervatamia divaricata* leaf extracts were reported by Ail *et al.* [9]. Vincristine and vinblastine from *Catharanthus roseus* have been used in cancer chemotherapy [10].

Many species in the Apocynaceae family are known in different parts of the world as toxic and/or medicinal. The poisonous plant database from the U.S. Food and Drug Administration (FDA, www.accessdata.fda.gov/scripts/), some poisonous plants and poisonous parts have recorded in volumes 63 of the *Flora of China*, including *Strophanthus hispidus*, *Cerbera manghas*, *Thevetia peruviana*, and *Nerium oleander*. The seeds of *Thevetia peruviana* cause dizziness, vomiting, and cardiac dysrhythmias upon ingestion, as reported by Eddleston *et al.* [11]. *Nerium oleander* contains a mixture of very toxic cardiac glycosides that cause poisoning *via* the inactivation of Na^+ and K^+ ATPases in the plasma membrane of cardiac myocytes [12]. The toxic effects of oleander have been reported in horses, cattle, sheep, goats, dogs, cats, birds, humans, donkeys, camels, monkeys, budgerigars, geese, ducks, turkeys, toed sloths and bears [13-15]. Toxic and potent medicines are irreplaceable in the treatment of some diseases. However, it is easy to cause serious poisoning events or even endanger the lives of patients if the identification is wrong. To ensure the safety of medications, it is vital to accurately identify species within the Apocynaceae family.

In traditional methods, such as morphological authentication, the identification of species is based on morphological characteristics [16]. However, traditional taxonomy research usually requires the expertise of an experienced professional taxonomist. As morphological features are always influenced by environmental and other factors, it is difficult for even a professional taxonomist to identify a species correctly. *Plumeria rubra* as an herbal material is easily confused with dry flowers of *Bombax ceiba*, *Campsis grandiflora*, *Campsis radicans*, *Tecomaria capensis*, and *Erythrina crista-galli* due to morphological similarities. In particular, the morphology of flowers has a large degree of shrinkage and fragmentation, rendering their differentiation very difficult and sometimes impossible [17]. Due to the challenging taxonomic identification of *Rauvolfia serpentina* sterile roots, Eurlings *et al.* successfully revealed the taxonomic identity of a sterile root sample using *rps16* [18]. Chemical profiling, such as high-performance liquid chromatography (HPLC) [19] and thin-layer chromatography (TLC) [20], can be used to qualitatively and quantitatively detect the constituents to identify herbal medicinal plants. However, these methods can have difficultly identifying closely related species that share remarkably similar or identical morphological characteristics and chemical profiles [21]. Chemical analysis techniques provide indirect evidence of fraud and cannot definitively determine the identity of the adulterated species [22]. However, DNA barcoding overcomes the problems associated with morphological identification and is used not only to correctly identify specimens and closely related species but also to discover new species [23, 24]. Compared with other molecular identification methods, DNA barcoding has good repeatability, high stability and strong universality, which might support the construction of a unified database and identification platform. The nuclear internal transcribed spacer 2 (ITS2) and the chloroplast *psbA-trnH* intergenic region have been used as suitable universal barcodes to identify medicinal plants and their closely related species [25-30]. In 2010, Chen *et al.* proposed that *psbA-trnH* can be used as a supplementary marker for the differentiation of medicinal plants [31]. Cabelin and Alejandro applied *trnH-psbA* and *trnL-F* as supplementary barcodes to *matK* for species identification of Philippine ethnomedicinal Apocynaceae [32]. The *trnH-psbA* and *matK* as core DNA barcodes were used to identify species for medicinal plants of Rauvolfioideae from northeast India [33]. ITS2 was applied accurately and effectively to distinguish the herbal tea ingredient *Plumeria rubra* from its adulterants [17]. Yu *et al.* applied ITS2 as a candidate DNA barcode to identify and distinguish *Trachelospermum jasminoides* from its local alternatives, including *Ficus pumila*, *Ficus tikoua*, and *Euonymus fortune* [34]. Although many reports have validated the reliability of ITS2 for authenticating medicinal plants and their adulterants, molecular identification based on the ITS2 barcode using experimental data has not yet been completed for the family Apocynaceae.

In the present study, we employed the ITS2 and *psbA-trnH* regions to authenticate species of the Apocynaceae family. Additionally, important toxic genera, such as *Allamanda*, *Alstonia*, *Catharanthus*, *Cerbera*, *Ervatamia*, *Strophanthus*, *Trachelospermum*, *Nerium*, *Rauwolfia*, and *Thevetia*, were examined for genetic and phyletic variations using DNA barcode loci.

Materials and Methods

Plant materials and sequence collection

A total of 122 samples of 31 species from 19 genera were collected. All plant species were identificated by professional botanist LI Hai-Tao (Yunnan Branch, Institute of Medicinal Plant Development, Chinese Academy of Medical Sciences & Peking Union Medical College) and LIN Yu-Lin (Institute of Medicinal Plant Development, Chinese Academy of Medical Sciences & Peking Union Medical College), respectively. The fresh leaves of the plant were collected from the Xishuangbanna South Medicinal Plant Garden of Jinghong (Yunnan Province, China) and the Medicinal Botanical Garden of Nanning (Guangxi Province, China) and were dried immediately using silica gels for DNA extraction, while the dried stem samples were purchased from Traditional Chinese Medicine Market (Table S2). Description of experimental samples is provided in the (Table S2). The voucher specimen for each species is curated in the Herbarium. Apocynum venetum is deposited in the Herbarium of the Institute of Medicinal Plant Development (IMD), Chinese Academy of

Medical Sciences (CAMS). All other corresponding voucher specimens are deposited in the Herbarium of the Yunnan Branch of the Institute of Medicinal Plant Development (IMDY), Chinese Academy of Medical Sciences (Table S2). Additional data involved 51 sequences of the ITS2 region belonging to 11 species and 42 sequences of the *psbA-trnH* region belonging to 17 species, which were downloaded from GenBank (Table S3).

DNA extraction, amplification, and sequencing

The DNA extraction and amplifcation of the ITS2 and *psbA-trnH* locus of the 122 samples were conducted. Total DNA was extracted with a Plant Genome DNA Kit (Cat. #DP305, Tiangen Biotech (Beijing) Co., Ltd., China) in accordance with the manufacturer's instructions. To examine the efficiency of amplification for the ITS2 and *psbA-trnH* DNA barcodes, PCR with universal primers and conditions was performed using genomic DNA from 31 species in the family Apocynaceae as templates. PCR amplification of the ITS2 and *psbA-trnH* genes was accomplished using an A600 Gradient Thermal Cycler (LongGene Scientific Instruments Co., Ltd., China). The ITS2 and *psbA-trnH* regions were amplified using the following pairs of universal primers [31, 35]:

ITS-2F: 5′-ATGCGATACTTGGTGTGAAT-3′

ITS-3R: 5′-GACGCTTCTCCAGACTACAAT-3′

Fwd-PA: 5′-GTTATGCATGAACGTAATGCTC-3′

Rev-TH: 5′-CGCGCATGGTGGATTCACAATCC-3′

The PCR reactions were performed using a final volume of 50 μL for ITS2 and *psbA-trnH* markers: 1.25 U of Blend Taq®-Plus (Toyobo Co., Ltd., Japan), 0.2 mmol·L^{-1} dNTPs, 0.2 μmol·L^{-1} of each primer and 50 ng·μL^{-1} of genomic DNA template. The reaction conditions for ITS2 were 94 °C for 5 min, 40 cycles of 94 °C for 30 s, 60 °C for 30 s, and 72 °C for 45 s, followed by 72 °C for 10 min. The reactions conditions for *psbA-trnH* were 94 °C for 5 min, 35 cycles of 94 °C for 1 min, 60 °C for 1 min, and 72 °C for 1.5 min, followed by 72 °C for 7 min. The PCR products were sequenced bidirectionally by using ABI 3730XL automated sequencer (Beijing Sino Geno Max Co., Ltd.).

Sequence alignment and analysis

The original sequences were proofread and assembled using CodonCode Aligner V7.2.1 (CodonCode Co., USA). The ITS2 region was removed from the conserved 5.8S and 28S DNA sequences based on the ITS2 database web server (http://its2.bioapps.biozentrum.uni-wuerzburg.de). Average intraspecific distances, theta values and coalescent depths were calculated to determine intraspecific variation using a Kimura 2-parameter (K2P) distance model [24, 31]. Average interspecific distances, theta prime values and average minimum interspecific distances were used to characterize interspecific divergence [27, 31]. The distributions of intraspecific and interspecific variability were compared by using DNA barcoding gaps that refers to the 'gap' between interspecific variations and intraspecific variations [36, 37]. The six parameters were calculated by the Perl program and SigmaPlot 12.0 software (Systat Software, Inc, Point Richmond, CA). Neighbor-joining (NJ) trees were constructed based on Muscle alignment results (parameter settings showed in Table S4) according to the K2P model using MEGA 7.0.26 [(Sudhir Kumar , Glen St echer, and Koichiro Tamura (2015)] and performed with 1000 bootstrap replicates [38]. Species identification was implemented using the BLAST1 method, which was performed using the BLAST program (Version 2.2.17, Christiam Camacho, USA) and the distance-based method [39]. The BLAST1 method is based on the best hit of the query sequence that is all ITS2 sequences and *psbA-trnH* sequences of Apocynaceae species and the *E*-value for the match must be less than a cutoff value to determine the identity of a sample. The distance-based method is based on all pairwise genetic distances computed among the reference sequences, and between each query and each of the reference sequences, which determines the identity of a sample.

Secondary structure prediction and two-dimensional DNA barcoding

In order to deduce the usefulness of ITS2 secondary structure for species discrimination. We chose morphologically similar species of *Rauvolfia* for secondary structure prediction using the ITS2 Workbench (http://its2.bioapps.biozentrum.uni-wuerzburg.de/) [40]. Quick response (QR) code was a suitable symbology for the DNA barcode sequences. The ITS2 sequences of *Rauvolfia* were transformed into two-dimensional images using the QR Code coding approach (http://qrfordna.dnsalias.org) [41, 42].

Results

PCR amplification efficiency and sequence characteristics

To facilitate PCR amplification and DNA sequencing, the ITS2 and *psbA-trnH* gene sequences were amplified using a single pair of universal primers for each locus. The amplification rates of ITS2 sequences and *psbA-trnH* sequences were 100%. The sequencing success rates for ITS2 sequences and *psbA-trnH* sequences were 81% and 61%, respectively. The average length of the ITS2 sequences was 230 bp, ranging from 208 bp to 259 bp. The average GC content was 66%. The average length of the *psbA-trnH* sequences was 394 bp, with a range of 164 to 584 bp. The mean GC content was 26.0%.

Intra-specific and inter-specific genetic divergence analyses

First, three parameters were used to characterize intraspecific divergence: (i) average intraspecific difference, (ii) theta, and (iii) average coalescent depth. Here, the ITS2 region exhibited higher interspecific divergence than the *psbA-trnH* region, according to all three parameters (Table 1). Second, three additional parameters were used to determine intraspecific variation: (i) average interspecific difference, (ii) average theta prime, and (iii) average minimum interspecific distance. In comparisons of interspecific genetic distance between congeneric species using the ITS2 and *psbA-trnH* barcodes, the *psbA-trnH* region exhibited higher interspecific divergence than the ITS2 region, according to all three parameters (Table 1). The overall intraspecific distance,

Table 1 Metrics of interspecific and intraspecific divergence for ITS2 and *psbA-trnH*.

Measurement	ITS2	*psbA-trnH*
Average intraspecific distance	0.0027 ± 0.0081	0.0029 ± 0.0055
Theta	0.0057 ± 0.0096	0.0009 ± 0.0019
Average coalescent depth	0.0084 ± 0.0135	0.0026 ± 0.0060
Average interspecific distance	0.0420 ± 0.0528	0.231 ± 0.0385
Average theta prime	0.0504 ± 0.0524	0.283 ± 0.0421
Average minimum interspecific distance	0.0295 ± 0.0371	0.227 ± 0.0442

coalescent depth, interspecific distance, and minimum interspecific distance for each species are shown in Fig. 1. The intraspecific coalescent depth values of ITS2 and *psbA-trnH* were smaller than the minimum interspecific distance values, which showed that ITS2 and *psbA-trnH* could discriminate plants of the Apocynaceae family. In addition, the interspecific discriminatory ability of *psbA-trnH* was superior to that of ITS2.

Assessment of barcoding gaps

To investigate intraspecific and interspecific divergence, we scrutinized the distribution of genetic distance at a scale of 0.01 distance units. The barcoding gaps of ITS2 and *psbA-trnH* were not distinct (Fig. 2). Some of the samples were closely related to each other. For *psbA-trnH*, the interspecific divergence ranged from 0.000 to 0.190, with a value of zero for 2.839% of samples, and the intraspecific divergence ranged from 0.000 to 0.030. We used Wilcoxon two-sample tests, which showed significant differences between the interspecific and intraspecific divergences for ITS2 (P = 0.0000)

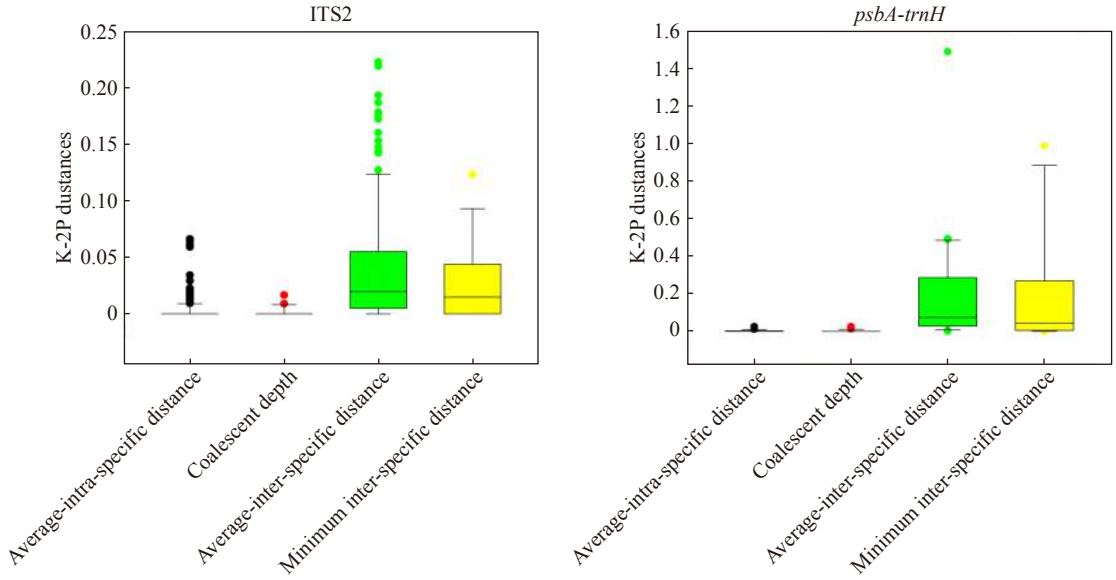

Fig. 1 Box plots of four parameters for the ITS2 and *psbA-trnH* sequences. In a box plot, the box shows the interquartile range (IQR) for the data. The IQR is defined as the difference between the 75th percentile and the 25th percentile. The solid line through the box represents the average distance

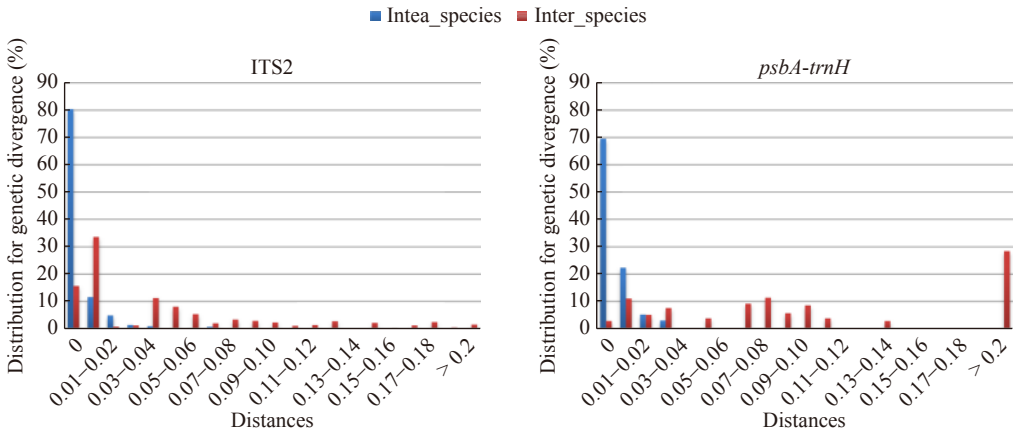

Fig. 2 Distribution of intra- and interspecific distances for the ITS2 and *psbA-trnH* regions among dataset sequences

and *psbA-trnH*. (P = 0.0001). The barcode gap analysis revealed a partial overlap between the intraspecific and interspecific distances of ITS2 and *psbA-trnH*. The interspecific distances of sequences for ITS2 and *psbA-trnH* were considerably higher than the intraspecific distances (Fig. 1). Moreover, the mean interspecific distances were significantly higher than the corresponding intraspecific distances for both ITS2 and *psbA-trnH* regions (Table 1).

Authentication efficiency analysis

To test the authentication efficiency of ITS2 and *psbA-trnH* for Apocynaceae samples, the BLAST1 and distance-based methods were selected. In the BLAST1 method, ITS2 showed a high identification efficiency of 97% and 100% of the samples at the species and genus levels, respectively. *psbA-trnH* showed identification efficiency of 95% and 100% at the species and genus levels, respectively (Table 2). In addition, the barcode combination of ITS2/*psbA-trnH* correctly identified 98% and 100% of the samples at the species and genus levels, respectively, which is based on "traffic light method" [43]. In DISTANCE method, ITS2 showed identification efficiency of 86% at the species level, and *psbA-trnH* showed identification efficiency of 82% at the species level (Table 2). Thus, all of the above results clearly suggested that ITS2 possesses a slight higher success rate than *psbA-trnH* for species and genus identification. ITS2 might better distinguish the plants of the Apocynaceae family. The *psbA-trnH* region was thus used as a complementary barcode

In addition, the NJ tree was constructed to distinguish the medicinally important plants of the Apocynaceae based on all 151 sequences of the ITS2 region, including 100 sequences from experimental samples and 51 sequences downloaded from GenBank. The NJ tree showed that most species could be discriminated (Fig. 3). For example, morphologically similar species of *Rauvolfia* like *Rauvolfia verticillata*, *Rauvolfia perakensis*, *Rauvolfia yunnanensis*, *Rauvolfia sumatrana*, *Rauvolfia serpentine*, *Rauvolfia tetraphylla*, *Rauvolfia vomitoria* were clearly distinguished by the region ITS2 (Figs. 3, 4 and 5). In Fig. 4, the secondary structures of ITS2 regions of 7 *Rauvolfia* species were predicted to identify species. All ITS2 secondary structures exhibited a central ring and four similar helices, namely, Helix I, II, III, and IV. The secondary structure of 7 *Rauvolfia* species was similar but different from each other in the position, size, and number of loops on Helix I, III and IV, which can provide another dimensionality to identify *Rauvolfia* species at the molecular morphological characteristics level (Fig. 4). In Fig. 5, the ITS2 sequences of *Rauvolfia* were based on the open source PHP QR code, and *Rauvolfia* species information was captured by scanning the QR code image using a mobile terminal and submitted to the system for confirmation. The Fig. 5 only shows sequence characteristics of ITS2 sequence dominant haplotype of 7 *Rauvolfia* species. Only a few species could not be identified, including 3 groups: *Trachelospermum jasminoides* and *Trachelospermum jasminoides* var. *jasminoides*, *Allamanda. cathartica* and *Allamanda blanchetii*; *Ervatamia divaricata* and *Ervatamia flabelliformis*. The NJ tree for *psbA-trnH* sequences showed that most species could be discriminated based on 117 sequences, including 75 sequences from experimental samples and 42 sequences downloaded from GenBank (Fig. 6). Compared with NJ tree for ITS2 and *psbA-trnH*, *Allamanda cathartica* and *Allamanda blanchetii* samples were not effectively identified using the ITS2 barcode but could be effectively distinguished based on the *psbA-trnH* barcode.

The ITS2 mark should show variation to differentiate the genetic and phyletic relationships of 10 toxic genera: *Allamanda*, *Alstonia*, *Catharanthus*, *Cerbera*, *Ervatamia*, *Nerium*, *Strophanthus*, *Trachelospermum*, *Rauwolfia*, *and Thevetia*. For the samples collected, using ITS2 for species identification resulted in a 100% success rate for these genera. The success rate of ITS2 for species identification in these species was 86%. In Fig. 3, 10 toxic genera are noted with red. 10 toxic species, including *Allemanda neriifolia*, *Cerbera manghas*, *Rauvolfia serpentina*, *Rauvolfia verticillata*, *Rauvolfia tetraphylla*, *Rauvolfia vomitoria*, *Thevetia peruviana*, *Catharanthus roseus*, *Strophanthus divaricatus*, and *Nerium indicum* were clearly distinguished by the ITS2 region, and information on the morphologically similar species *Rauvolfia serpentina*, *Rauvolfia verticillata*, *Rauvolfia tetraphylla* and *Rauvolfia vomitoria* can be obtained by scanning

Table 2 Identification success rates of ITS2 and *psbA-trnH* regions in Apocynaceae samples using BLAST1 and distance-based methods

Marker	No. of genera	No. of species	No. of samples	Method of species identification	Plant taxalevel	Correct efficiency/%
ITS2	19	37	151	BLAST	genus	100
					species	97
				Distance	genus	96
					species	86
psbA-trnH	17	28	113	BLAST	genus	100
					species	95
				Distance	genus	95
					species	82

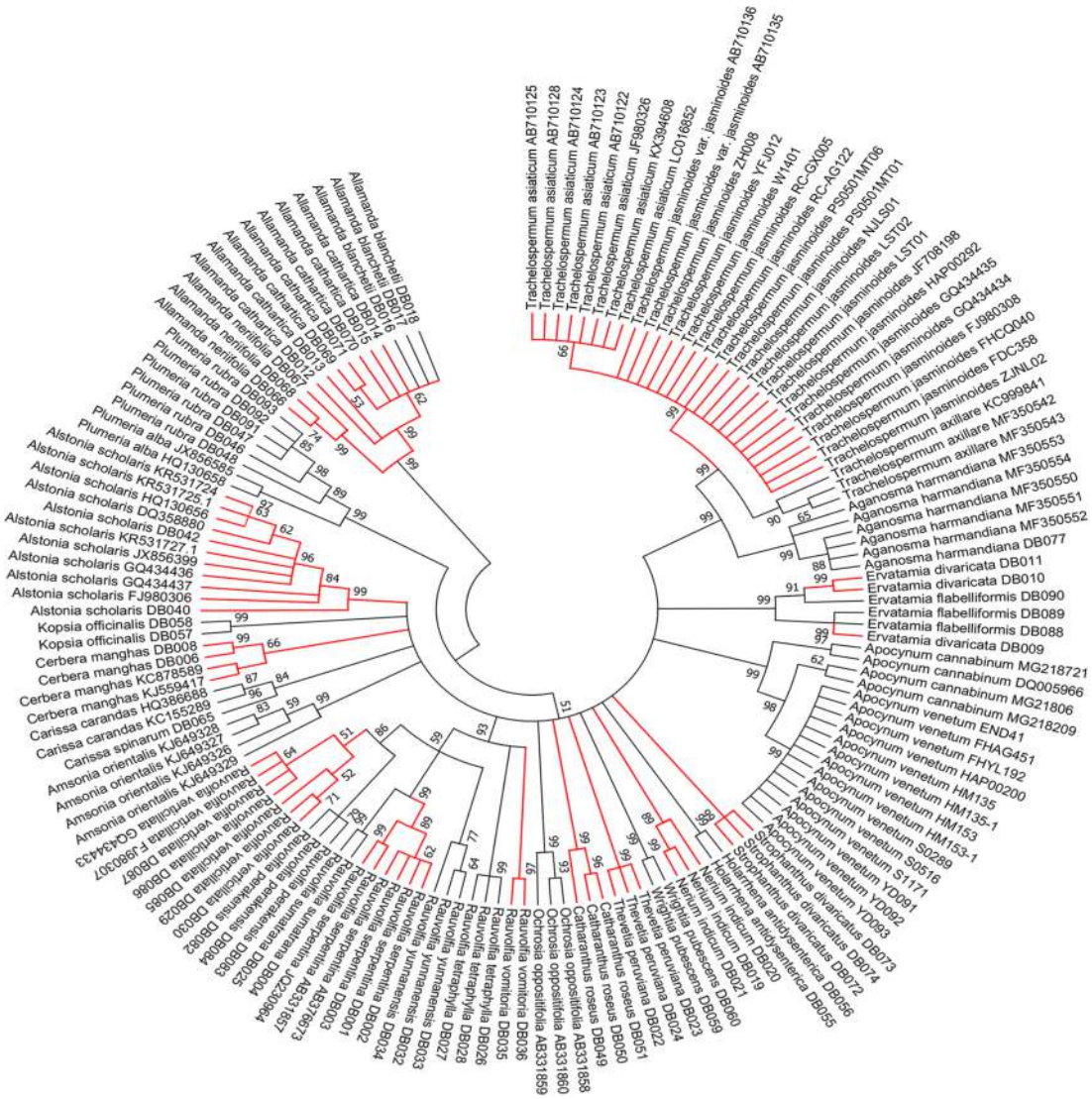

Fig. 3 Phylogenetic tree constructed based on the ITS2 regions. Results from neighbor-joining (NJ) bootstrap analyses with 1000 replicates was used to assess the strength of the nodes. The node numbers indicated the bootstrap value of NJ. The red represents toxic species

the QR code image using a mobile terminal and submitted to the system for confirmation (Fig. 5).

Discussion

First identification of species in the apocynaceae family by ITS2 based on experimental data

The ITS2 locus, a relatively short segment belonging to the ITS region, has been widely adopted as an efficient DNA barcode for the identification of medicinal plants and their closely related species [31]. The ITS2 region is much shorter than the full ITS region and is a good choice because of its conserved sequence, which can be amplified and sequenced more easily than the full ITS region for various medicinal plants. In a study by Selvaraj *et al.* 70% of the ITS fragments (15 species) of the 21 species were successfully amplified in the Apocynaceae family [44]. Although the ITS sequence contains enough variable sites to determine the species in many samples [45, 46], approximately 12% of herbarium samples could not be amplified using the ITS primer [47, 48]. In 2013, Han *et al.* showed that ITS2 exhibited 91% efficiency while ITS exhibited only 23% efficiency in PCR, based on 1260 samples from dry medicinal products and herbarium voucher specimens, including some samples collected up to 90 years ago [49]. Compared to the results from the study by Selvaraj *et al.* our experimental results showed that ITS2 is easily amplified and sequenced with a greater success rate than ITS sequences in the Apocynaceae family. In addition, in 2010, Yao *et al.* showed that ITS2 could be used as a universal DNA barcode for identifying plants using bioinformatics analysis [38].

Selvaraj *et al.* have also shown that *matK* and *rbcL* showed 90% and 85% of amplification efficiency in Apocynaceae species, respectively [44], whereas ITS2 exhibited 100% for the plant species of Apocynaceae in our experimental analysis. They have also proven that *matK* and *rbcL* were less

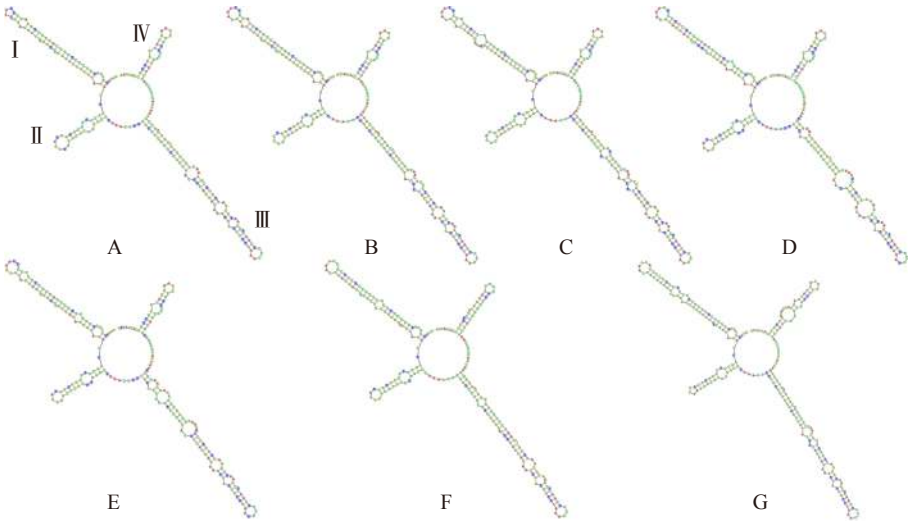

Fig. 4 Secondary structure of ITS2 in seven *Rauvolfia* species. (A) *Rauvolfia verticillata*; (B) *Rauvolfia perakensis*; (C) *Rauvolfia yunnanensis*; (D) *Rauvolfia sumatrana*; (E) *Rauvolfia serpentina*; (F) *Rauvolfia tetraphylla*; (G) *Rauvolfia vomitoria*

powerful than ITS2 in Apocynaceae species discrimination.

Altogether, our results demonstrate that both ITS2 and *psbA-trnH* are powerful loci for differentiating species within Apocynaceae. Based on previous reports and our own findings, we proposed that ITS2 could provide rapid and reliable species identification and be used as the preferred barcode for species within the Apocynaceae family according to our experimental analyses, in addition, secondary structures of ITS2 could provide additional variation information for distinguishing closely related species and morphologically similar species. Meanwhile, we propose that *psbA-trnH* could be used as a supplementary barcode for differentiating those species within the Apocynaceae family that cannot be identified by ITS2.

The identification of the Apocynaceae family has the potential to significantly enrich DNA barcoding reference databases

DNA barcoding can be used as a new effective technology for medicinal plant authentication in traditional medicine, which is important for the clinical safety of medications and commercial products. The "aristolochic acid nephropathy (AAN)" incident is world-famous and was caused by aristolochic acid [50], which is found in many Aristolochiaceae species, including *Aristolochia manshuriensis*, *Aristolochia mollissima*, and other species of the same genus. To avoid the health risks of aristolochic acid (AA), Wu *et al.* provided a DNA barcoding-based authentication system that could efficiently and reliably distinguish Aristolochiaceous materials from non-Aristolochiaceous materials [50]. In addition, researchers have successfully built some DNA barcode reference libraries for herbal drugs. For example, in 2010, Lou *et al.* created the first Medicinal Materials DNA Barcode Database (MMDBD) (http://www.cuhk.edu.hk/icm/mmdbd.htm), which contains 62 011 sequences from 2111 species [51]. In 2014, a preliminary system for the DNA barcoding of herbal materials (http://www.tcmbarcode.cn/en/) was constructed by Chen *et al.*, this system contains 78 847 sequences belonging to 23 262 species [52]. In 2017, Chen *et al.* established an online DNA barcode identification system (http://www.jpbarcode.com), that contains standard barcode sequences from approximately 95% of the species included in the Japanese Pharmacopoeia [53]. Liu *et al.* developed a DNA barcode reference library for monitoring herbal drugs in the Korean Pharmacopoeia, which contains 30 744 sequences (ITS2 and *psbA-trnH*) from 1054 specimens [54]. To prevent the occurrence of events or problems similar to AAN, species of the Apocynaceae family were distinguished based on ITS2 and *psbA-trnH*, which might supplement and improve population coverage for the above DNA barcoding reference databases that contain nearly all herbal drugs and other medicinal materials; in particular, some poisonous medicinal species of the Apocynaceae family were identified, including *Aganosma harmandiana*, *Alstonia scholaris*, *Allemanda neriifolia*, *Cerbera manghas*, *Rauvolfia serpentina*, *Rauvolfia verticillata*, *Rauvolfia vomitoria*, *Thevetia peruviana*, *Catharanthus roseus*, *Strophanthus divaricatus*, *Trachelospermum asiaticum*, *Nerium indicum*. At present, the most frequently used methods for chemical constituent and quality analysis of traditional Chinese medicines (TCMs) are various chromatographic and spectroscopic methods [55, 56]. However, these quality control approaches only measure the chemicals of interest and are not sufficient for ensuring the presence of authentic herbal ingredients or detection of contaminants/adulterants. DNA barcoding technology for TCM has been included in the Chinese and British pharmacopoeias [57], and has become the international standard for TCM identification. DNA barcoding technology combined with high-throughput technology may become a powerful tool for the quality control of TCM [58-61]. Xin *et al.* accurately identified herbal ingredients of Longdan Xiegan Wan (LDXGW) using DNA barcoding (ITS2 and *psbA-trnH* regions) and shotgun metagenomic sequencing and detected the substitution of *Akebiae*

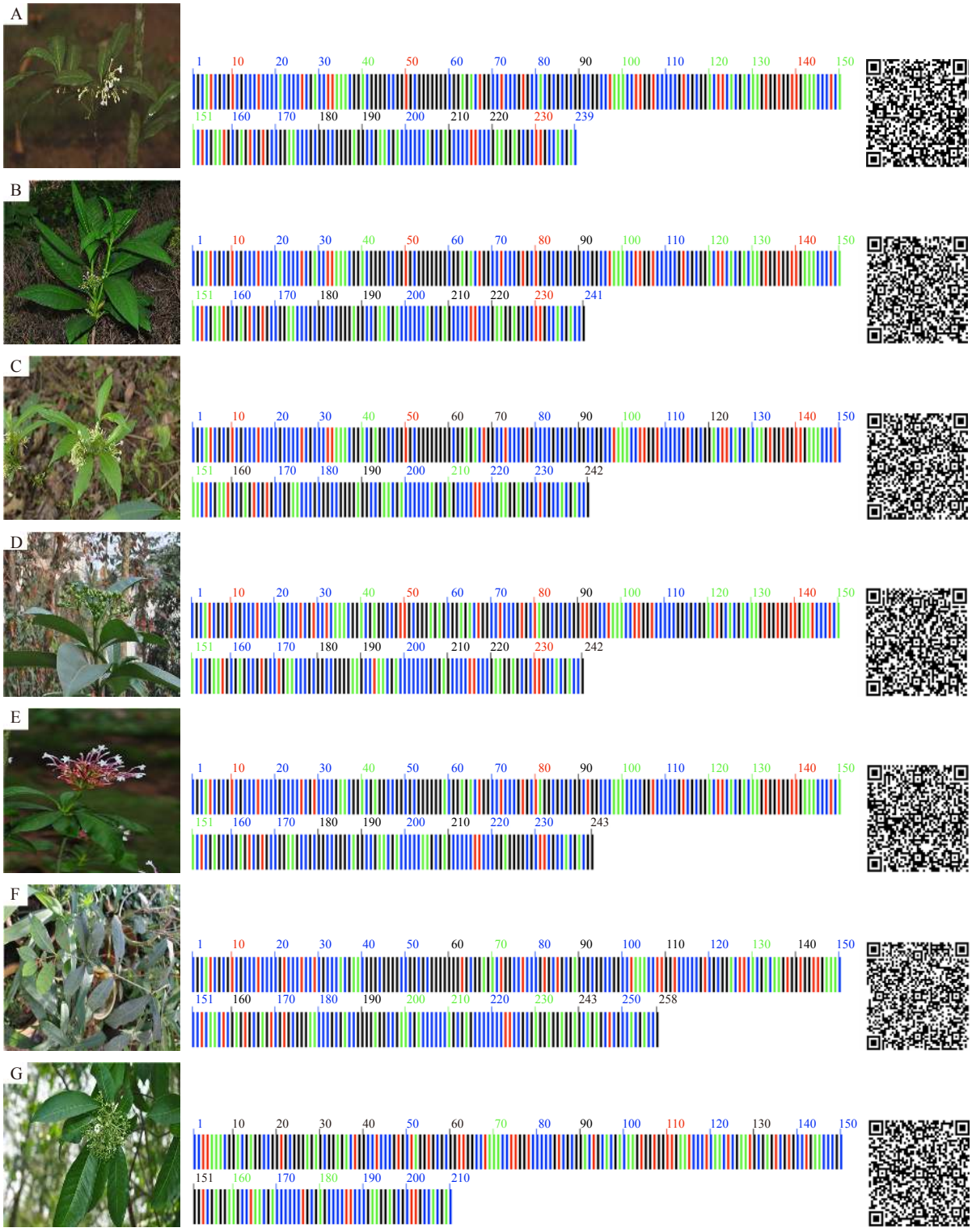

Fig. 5 Seven *Rauvolfia* species morphology, DNA barcoding and two-dimensional DNA barcoding image of ITS2 sequences. (A) *Rauvolfia verticillata*; (B) *Rauvolfia perakensis*; (C) *Rauvolfia yunnanensis*; (D) *Rauvolfia sumatrana*; (E) *Rauvolfia serpentine*; (F) *Rauvolfia tetraphylla*; (G) *Rauvolfia vomitoria*. In the center colored DNA image, the different colors represent different nucleotides (A ■ T ■ C ■ G ■) and the numbers represent the lengths of the sequences, which can be used in obtaining clear sequence information

Caulis (Mutong) in commercial samples, while chemical analyses could not [62], in addition, the herb "Mu tong" has been successfully identified using short fragments of ITS2 sequences with their secondary structure in previous studies [63].

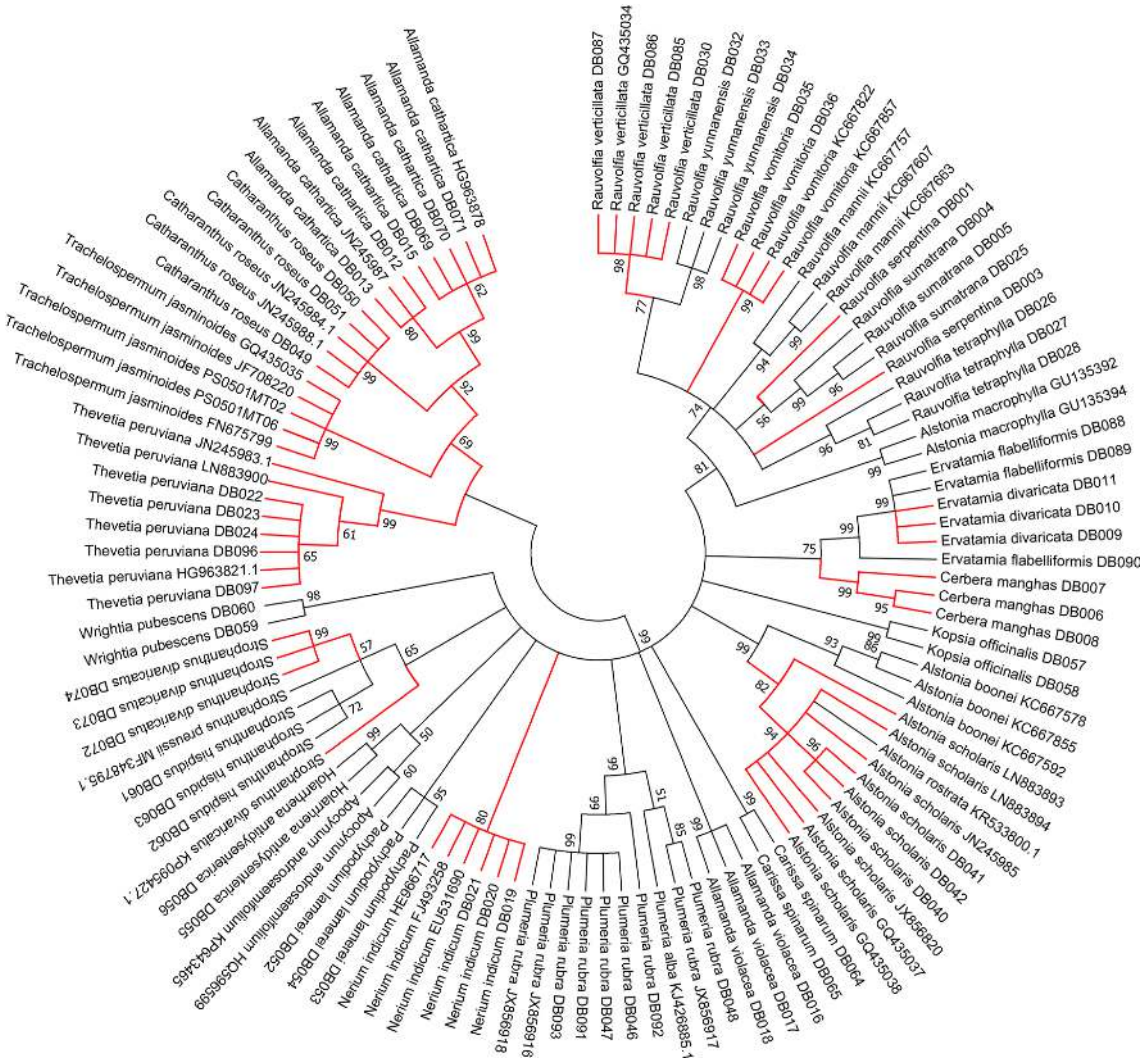

Fig. 6 Phylogenetic tree constructed based on the *psbA-trnH* regions. Results from neighbor-joining (NJ) bootstrap analyses with 1000 replicates was used to assess the strength of the nodes. The node numbers indicated the bootstrap value of NJ. The red represents toxic species

Jia *et al.* [64] and Xin *et al.* [65] performed preliminary studies of traditional Chinese patent medicines (THMPs), separately employing DNA barcoding (ITS2 and *psbA-trnH* regions) and single-molecule real-time (SMRT) sequencing. They demonstrated the application of SMRT sequencing to detect multiple biological ingredients of THMPs. In addition, the combination of DNA barcoding and chemical analysis could have the added advantage of comprehensive quality assessment of TCM, which is necessary for quality control. For example, Wei *et al.* established an integrated evaluation system based on ITS2 and LC-MS/MS to identify species and quantitative analysis for Uncaria medicinal materials. We hope that these research results will help to develop and perfect DNA barcoding reference databases for herbal drugs and other herbal raw materials.

Challenges and potential of the ITS2 barcode for the Apocynaceae family

The remaining 3% of samples could not be accurately identified at the species level; among these samples, no mutated site could be discovered in *Ervatamia divaricata* and *Ervatamia flabelliformis*. The Latin name of *Ervatamia flabelliformis* was recently changed to *Ervatamia divaricata* in the English edition of the *Flora of China*. Therefore, *Ervatamia divaricata* and *Ervatamia flabelliformis* were classified as the same species. In addition, *Allamanda cathartica* and *Allamanda blanchetii* samples were not effectively identified using the ITS2 barcode but could be effectively distinguished based on the *psbA-trnH* barcode. Interestingly, Chaveerach *et al.* adopted inter-simple sequence repeat (ISSR) analyses to clearly distinguish species of the genus *Allamanda*, such as *Allamanda cathartica* and *Allamanda blanchetii*, in 2014 [66]. Moreover, Yao *et al.* found that *psbA-trnH* could distinguish various *Dendrobium* species and adulterating species [38]. Han *et al.* showed that *psbA-trnH* sequences were significantly different in the intrespecific variation between *Cistanche* species and other morphologically

undistinguishable species [67]. In addition, compared with other chloroplast markers, the interspecific divergence of the *psbA-trnH* locus is higher than that of other plastid loci investigated, even though the *matK* locus demonstrates only half of the interspecific divergence of the *psbA-trnH* locus [35, 68, 69]. The *psbA-trnH* region has shown high variability and could be used to illuminate genetic relationships at the intraspecific level [70]. For example, in a study by Hamilton *et al. trnH-psbA* regions were highly variable and showed 15% divergence within the Lecythidaceae [71].

For land plants, many DNA barcodes have been evaluated, but identifying closely related or recently evolved species, especially within species-rich genera, remains a major challenge [72, 73]. In our study, *Trachelospermum jasminoides* and *Trachelospermum jasminoides* var. *jasminoides*, exhibited small genetic distances, and the mutation rate was 0%. DNA barcodes do not correctly distinguish recently diverged species, which may be due to incomplete or poor "barcode gaps"; this characteristic is related to the effective population size and the low evolutionary rate of the species [74]. The chloroplast genome is ideal for ecological, evolutionary, and diversity studies, which is important for providing subspecies- or variety-level resolution [75-79]. The complete chloroplast genome is very useful for identifying unclear phylogenetic relationships. For example, Zhu *et al.* accurately authenticated of *Dendrobium officinale* and its closely related species using the complete plastome sequences [80]. Therefore, the positive results in these studies suggested that we should attempt to discriminate *Trachelospermum jasminoides* and its closely related species using the chloroplast genome in future studies.

Conclusion

In summary, our experimental results suggested that ITS2 and *psbA-trnH* could provide rapid and reliable species identification and be used as the preferred barcode for species within the Apocynaceae family.

Appendix A. Supplementary data

Table S1−S4 are available as Supporting Information, and can be requested by sending E-mail to the corresponding author.

References

[1] Bhadane BS, Patil MP, Maheshwari VL, *et al*. Ethnopharmacology, phytochemistry, and biotechnological advances of family Apocynaceae: A review [J]. *Phytother Res*, 2018, **32**(7): 1181-1210.

[2] Zhang J, Li H, Li Y, *et al*. Four new corynanthe-type alkaloids from the roots of *Alstonia scholaris* [J]. *Chin J Nat Med*, 2019, **17**(12): 918-923.

[3] Fu LW, Zhang SJ, Li N, *et al*. Three new triterpenes from *Nerium oleander* and biological activity of the isolated compounds [J]. *J Nat Prod*, 2005, **68**(2): 198-206.

[4] Wong SK, Lim YY, Ling SK, *et al*. Caffeoylquinic acids in leaves of selected Apocynaceae species: Their isolation and content [J]. *Pharmacognosy Res*, 2014, **6**(1): 67-72.

[5] Deng Y, Bao MF, Shi BB, *et al*. Three new indole alkaloids from *Tabernaemontana divaricata* [J]. *Nat Prod Bioprospect*, 2018, **8**(3): 183-188.

[6] Wang CH, Wang GC, Wang Y, *et al*. Cytotoxic dimeric indole alkaloids from *Catharanthus roseus* [J]. *Fitoterapia*, 2012, **83**(4): 765-769.

[7] Ali Khan MS, Mat Jais AM, Afreen A. Prostaglandin analogous and antioxidant activity mediated gastroprotective action of *Tabernaemontana divaricata* (L.) R. Br. flower methanolic extract against chemically induced gastric ulcers in rats [J]. *Biomed Res Int*, 2013, **2013**: 185476.

[8] Botelho AFM, Santos-Miranda A, Joca HC, *et al*. Hydroalcoholic extract from *Nerium oleander* L. (Apocynaceae) elicits arrhythmogenic activity [J]. *J Ethnopharmacol*, 2017, **206**: 170-177.

[9] Jain S, Sharma P, Ghule S, *et al*. *In vivo* anti-inflammatory activity of *Tabernaemontana divaricata* leaf extract on male albino mice [J]. *Chin J Nat Med*, 2013, **11**(5): 472-476.

[10] Sharma A, Verma P, Mathur A, *et al*. Overexpression of tryptophan decarboxylase and strictosidine synthase enhanced terpenoid indole alkaloid pathway activity and antineoplastic vinblastine biosynthesis in *Catharanthus roseus* [J]. *Protoplasma*, 2018, **255**(5): 1281.

[11] Eddleston M, Persson H. Acute plant poisoning and antitoxin antibodies [J]. *J Toxicol Clin Toxicol*, 2003, **41**(3): 309-315.

[12] Wong A, Greene SL. Successful treatment of *Nerium oleander* toxicity with titrated Digoxin Fab antibody dosing [J]. *Clin Toxicol (Phila)*, 2018, **56**(7): 678-680.

[13] Adam SE, Al-Yahya MA, Al-Farhan AH. Toxicity of *Nerium oleander* and *Rhazya stricta* in Najdi sheep: hematologic and clinicopathologic alterations [J]. *Am J Chin Med*, 2002, **30**(2-3): 255-262.

[14] Kozikowski TA, Magdesian KG, Puschner B. Oleander intoxication in new world camelids: 12 cases (1995-2006) [J]. *J Am Vet Med Assoc*, 2009, **235**(3): 305-310.

[15] Ramesha A, Venkataramana M, Nirmaladevi D, *et al*. Cytotoxic effects of oosporein isolated from endophytic fungus Cochliobolus kusanoi [J]. *Front Microbiol*, 2015, **6**: 870.

[16] Vandebroek I. The identification of medicinal plants. A handbook of the morphology of botanicals in commerce by wendy applequest [J]. *Econ Bot*, 2006, **61**(3): 308-309.

[17] Shi YH, Sun W, Fang GH, *et al*. Identification of herbal tea ingredient *Plumeria rubra* and its adulterants using DNA barcoding [J]. *China J Chin Mater Med*, 2014, **39**(12): 2199-2203.

[18] Eurlings MC, Lens F, Pakusza C, *et al*. Forensic identification of Indian snakeroot (*Rauvolfia serpentina* Benth. ex Kurz) using DNA barcoding [J]. *J Forensic Sci*, 2013, **58**(3): 822-830.

[19] van Beek TA, Montoro P. Chemical analysis and quality control of *Ginkgo biloba* leaves, extracts, and phytopharmaceuticals [J]. *J Chromatogr A*, 2009, **1216**(11): 2002-2032.

[20] Kim HJ, Jee EH, Ahn KS, *et al*. Identification of marker compounds in herbal drugs on TLC with DART-MS [J]. *Arch Pharm Res*, 2010, **33**(9): 1355-1359.

[21] Han JP, Pang XH, Liao BS, *et al*. An authenticity survey of herbal medicines from markets in China using DNA barcoding [J]. *Sci Rep*, 2016, **6**: 18723.

[22] Mohammed AB, Mohd SF. Review: DNA barcoding and chromatography fingerprints for the authentication of botanicals in herbal medicinal products [J]. *Evid Based Complement Alternat Med*, 2017, **2017**: 1352948.

[23] Savolainen V, Cowan R, Vogler A, *et al*. Towards writing the encyclopaedia of life: an introduction to DNA barcoding [J]. *Philos Trans R Soc Lond B Biol Sci*, 2005, **360**(1462): 1805-1811.

[24] Schindel DE, Miller SE. DNA barcoding a useful tool for taxonomists [J]. *Nature*, 2005, **435**(7038): 17.

[25] Newmaster SG, Fazekas AJ, Steeves RA, *et al*. Testing candidate plant barcode regions in the Myristicaceae [J]. *Mol Ecol Resour*, 2008, **8**(3): 480-490.
[26] Song JY, Yao H, Li Y, *et al*. Authentication of the family Polygonaceae in Chinese pharmacopoeia by DNA barcoding technique [J]. *J Ethnopharmacol*, 2009, **124**(3): 434-439.
[27] Gao T, Yao H, Song JY, *et al*. Identification of medicinal plants in the family Fabaceae using a potential DNA barcode ITS2 [J]. *J Ethnopharmacol*, 2010, **130**(1): 116-121.
[28] Yang JB, Wang YP, Moller M, *et al*. Applying plant DNA barcodes to identify species of *Parnassia* (Parnassiaceae) [J]. *Mol Ecol Resour*, 2012, **12**(2): 267-275.
[29] Liu M, Li XW, Liao BS, *et al*. Species identification of poisonous medicinal plant using DNA barcoding [J]. *Chin J Nat Med*, 2019, **17**(8): 585-590.
[30] Hu SJ, Hu HY, Gao H, *et al*. DNA barcoding and rapid identification of the precious herb Herba Anoectochili [J]. *Chin J Nat Med*, 2019, **17**(10): 738-745.
[31] Chen SL, Yao H, Han JP, *et al*. Validation of the ITS2 region as a novel DNA barcode for identifying medicinal plant species [J]. *PLoS One*, 2010, **5**(1): e8613.
[32] Cabelin VL, Alejandro GJ. Efficiency of *matK*, *rbcL*, *trnH-psbA*, and *trnL-F* (cpDNA) to molecularly authenticate philippine ethnomedicinal apocynaceae through DNA barcoding [J]. *Pharmacogn Mag*, 2016, **12**(Suppl 3): S384-388.
[33] Mahadani P, Sharma GD, Ghosh SK. Identification of ethnomedicinal plants (Rauvolfioideae: Apocynaceae) through DNA barcoding from northeast India [J]. *Pharmacogn Mag*, 2013, **9**(35): 255-263.
[34] Yu N, Wei YL, Zhang X, *et al*. Barcode ITS2: a useful tool for identifying *Trachelospermum jasminoides* and a good monitor for medicine market [J]. *Sci Rep*, 2017, **7**(1): 5037.
[35] Kress WJ, Erickson DL. A two-locus global DNA barcode for land plants: the coding *rbcL* gene complements the non-coding *trnH-psbA* spacer region [J]. *PLoS One*, 2007, **2**(6): e508.
[36] Meyer CP, Paulay G. DNA barcoding: error rates based on comprehensive sampling [J]. *PLoS Biol*, 2005, **3**(12): e422.
[37] Meier R, Zhang GY, Ali F. The use of mean instead of smallest interspecific distances exaggerates the size of the "barcoding gap" and leads to misidentification [J]. *Syst Biol*, 2008, **57**(5): 809-813.
[38] Yao H, Song JY, Ma XY, *et al*. Identification of Dendrobium species by a candidate DNA barcode sequence: the chloroplast *psbA-trnH* intergenic region [J]. *Planta Med*, 2009, **75**(6): 667-669.
[39] Ross HA, Murugan S, Li WL. Testing the reliability of genetic methods of species identification via simulation [J]. *Syst Biol*, 2008, **57**(2): 216-230.
[40] Merget B, Koetschan C, Hackl T, *et al*. The ITS2 database [J]. *J Vis Exp*, 2012, **61**: 3806.
[41] Liu C, Shi LC, Xu XC, *et al*. DNA barcode goes two-dimensions: DNA QR code web server [J]. *PLoS One*, 2012, **7**(5): e35146.
[42] Xin TY, Li XW, Yao H, *et al*. A two-dimensional DNA barcode system for circulation regulation of traditional Chinese medicine [J]. *Sci Sin Vit*, 2015, **45**(7): 695-702.
[43] Chase MW, Salamin N, Wilkinson M, *et al*. Land plants and DNA barcodes: short-term and long-term goals [J]. *Philos Trans R Soc Lond B Biol Sci*, 2005, **360**(1462): 1889-1895.
[44] Selvaraj D, Sarma RK, Shanmughanandhan D, *et al*. Evaluation of DNA barcode candidates for the discrimination of the large plant family Apocynaceae [J]. *Plant Syst Evol*, 2015, **301**(4): 1263-1273.
[45] Doh EJ, Paek SH, Lee G, *et al*. Application of partial internal transcribed spacer sequences for the discrimination of *Artemisia capillaris* from other *Artemisia* species [J]. *Evid Based Complement Alternat Med*, 2016, **2016**: 7043436.
[46] Gogoi B, Bhau BS. DNA barcoding of the genus *Nepenthes* (Pitcher plant): a preliminary assessment towards its identification [J]. *BMC Plant Biol*, 2018, **18**(1): 153.
[47] Rubinoff D, Cameron S, Will K. Are plant DNA barcodes a search for the Holy Grail? [J]. *Trends Ecol Evol (Amst)*, 2006, **21**(1): 1-2.
[48] Liang LJ, Wang EH, Yang YC, *et al*. Study on hybrid characteristics of medicinally used cultivated codonopsis species using ribosomal internal transcribed spacer (ITS) sequencing [J]. *Molecules*, 2018, **23**(7): 1565.
[49] Han JP, Zhu YJ, Chen XC, *et al*. The short ITS2 sequence serves as an efficient taxonomic sequence tag in comparison with the full-length ITS [J]. *Biomed Res Int*, 2013, **2013**: 741476.
[50] Wu L, Sun W, Wang B, *et al*. An integrated system for identifying the hidden assassins in traditional medicines containing aristolochic acids [J]. *Sci Rep*, 2015, **5**: 11318.
[51] Lou SK, Wong KL, Li M, *et al*. An integrated web medicinal materials DNA database: MMDBD (Medicinal Materials DNA Barcode Database) [J]. *BMC Genomics*, 2010, **11**: 402.
[52] Chen SL, Pang XH, Song JY, *et al*. A renaissance in herbal medicine identification: from morphology to DNA [J]. *Biotechnol Adv*, 2014, **32**(7): 1237-1244.
[53] Chen XC, Xiang L, Shi LC, *et al*. Identification of crude drugs in the Japanese pharmacopoeia using a DNA barcoding system [J]. *Sci Rep*, 2017, **7**: 42325.
[54] Liu JX, Shi LC, Song JY, *et al*. BOKP: A DNA barcode reference library for monitoring herbal drugs in the Korean pharmacopeia [J]. *Front Pharmacol*, 2017, **8**: 931.
[55] Jiang Y, David B, Tu PF, *et al*. Recent analytical approaches in quality control of traditional Chinese medicines—A review [J]. *Anal Chim Acta*, 2010, **657**(1): 9-18.
[56] Jing J, Parekh HS, Ming W, *et al*. Advances in analytical technologies to evaluate the quality of traditional Chinese medicines [J]. *TrAC Trend Anal Chem*, 2013, **44**(44): 39-45.
[57] Commission TBPAXV. *Deoxyribonucleic Acid (DNA) Based Identification Techniques for Herbal Drugs* [M]. London: The British Pharmacopoeia Commission, 2015.
[58] Sgamma T, Lockie-Williams C, Kreuzer M, *et al*. DNA barcoding for industrial quality assurance [J]. *Planta Med*, 2017, **83**(14-15): 1117-1129.
[59] Gao ZT, Wang XY, Liu Y, *et al*. Identification of Chinese patent medicines containing *Fritillariae cirrhose* bulbus using ITS2 region (in chinese) [J]. *Sci Sin Vitae*, 2018, **48**(4): 482-489.
[60] Shi LC, Liu JX, Wei MJ, *et al*. DNA metabarcoding identification of prescription ingredients in traditional medicine Ruyi Jinhuang San (in Chinese) [J]. *Sci Sin Vitae*, 2018, **48**(4): 490-497.
[61] Xiong C, Sun W, Li J, *et al*. Identifying the species of seeds in traditional Chinese medicine using DNA barcoding [J]. *Front Pharmacol*, 2018, **9**: 701.
[62] Xin TY, Su C, Lin YL, *et al*. Precise species detection of traditional Chinese patent medicine by shotgun metagenomic sequencing [J]. *Phytomedicine*, 2018, **47**: 40-47.
[63] Zhang W, Yuan Y, Yang S, *et al*. ITS2 secondary structure improves discrimination between medicinal "Mu Tong" species when using DNA barcoding [J]. *PLoS One*, 2015, **10**(7): e0131185.
[64] Jia J, Xu Z, Xin T, *et al*. Quality control of the traditional patent medicine Yimu Wan based on SMRT sequencing and DNA barcoding [J]. *Front Plant Sci*, 2017, **8**: 926.
[65] Xin TY, Xu ZC, Jia J, *et al*. Biomonitoring for traditional herbal medicinal products using DNA metabarcoding and single

molecule, real-time sequencing [J]. *Acta Pharm Sin B*, 2018, **8**(3): 488-497.
[66] Chaveerach A, Aungkapattamagul S, Tanee T, *et al*. Genetic verification and chemical contents identification of *Allamanda* species (Apocynaceae) [J]. *Pak J Pharm Sci*, 2014, **27**(3): 417-424.
[67] Han JP, Song JY, Liu C, *et al*. Identification of *Cistanche* species (Orobanchaceae) based on sequences of the plastid *psbA-trnH* intergenic region [J]. *Acta Pharm Sin B*, 2010, **45**(1): 126-130.
[68] Hajibabaei M, Janzen DH, Burns JM, *et al*. DNA barcodes distinguish species of tropical Lepidoptera [J]. *Proc Natl Acad Sci U S A*, 2006, **103**(4): 968-971.
[69] Lahaye R, van der Bank M, Bogarin D, *et al*. DNA barcoding the floras of biodiversity hotspots [J]. *Proc Natl Acad Sci U S A*, 2008, **105**(8): 2923-2928.
[70] Azuma H, Garcia-Franco JG, Rico-Gray V, *et al*. Molecular phylogeny of the Magnoliaceae: the biogeography of tropical and temperate disjunctions [J]. *Am J Bot*, 2001, **88**(12): 2275-2285.
[71] Hamilton MB, Braverman JM, Soria-Hernanz DF. Patterns and relative rates of nucleotide and insertion/deletion evolution at six chloroplast intergenic regions in new world species of the Lecythidaceae [J]. *Mol Biol Evol*, 2003, **20**(10): 1710-1721.
[72] Liu J, Moller M, Gao LM, *et al*. DNA barcoding for the discrimination of *Eurasian yews* (Taxus L. Taxaceae) and the discovery of cryptic species [J]. *Mol Ecol Resour*, 2011, **11**(1): 89-100.
[73] Yan LJ, Liu J, Moller M, *et al*. DNA barcoding of *Rhododendron* (Ericaceae), the largest Chinese plant genus in biodiversity hotspots of the Himalaya-Hengduan Mountains [J]. *Mol Ecol Resour*, 2015, **15**(4): 932-944.
[74] van Velzen R, Weitschek E, Felici G, *et al*. DNA barcoding of recently diverged species: relative performance of matching methods [J]. *PLoS One*, 2012, **7**(1): e30490.
[75] Li QS, Li Y, Song JY, *et al*. High-accuracy de novo assembly and SNP detection of chloroplast genomes using a SMRT circular consensus sequencing strategy [J]. *New Phytol*, 2014, **204**(4): 1041-1049.
[76] He L, Qian J, Li XW, *et al*. Complete chloroplast genome of medicinal plant *Lonicera japonica*: genome rearrangement, intron gain and loss, and implications for phylogenetic studies [J]. *Molecules*, 2017, **22**(2): E249.
[77] Li Y, Zhou JG, Chen XL, *et al*. Gene losses and partial deletion of small single-copy regions of the chloroplast genomes of two hemiparasitic *Taxillus* species [J]. *Sci Rep*, 2017, **7**(1): 12834.
[78] Chen XL, Zhou JG, Cui YX, *et al*. Identification of Ligularia herbs using the complete chloroplast genome as a super-barcode [J]. *Front Pharmacol*, 2018, **9**: 695.
[79] Zhou JG, Cui YX, Chen XL, *et al*. Complete chloroplast genomes of *Papaver rhoeas* and *Papaver orientale*: molecular structures, comparative analysis, and phylogenetic analysis [J], Molecules, 2018, **23**(2): E437.
[80] Zhu SY, Niu ZT, Xue QY, *et al*. Accurate authentication of *Dendrobium officinale* and its closely related species by comparative analysis of complete plastomes [J]. *Acta Pharm Sin B*, 2018, **8**(6): 969-980.

Cite this article as: LV Ya-Na, YANG Chun-Yong, SHI Lin-Chun, ZHANG Zhong-Lian, XU An-Shun, ZHANG Li-Xia, LI Xue-Lan, LI Hai-Tao. Identification of medicinal plants within the Apocynaceae family using ITS2 and *psbA-trnH* barcodes [J]. *Chin J Nat Med*, 2020, **18**(8): 594-605.